International Journal of Nanomedicine

Dovepress
open access to scientific and medical research

Open Access Full Text Article

ORIGINAL RESEARCH

A novel albumin wrapped nanosuspension of meloxicam to improve inflammation-targeting effects

This article was published in the following Dove Press journal:
International Journal of Nanomedicine

Qi Li[1]
Fen Chen[2]
Yun Liu[1]
Shihui Yu[1]
Xiumei Gai[1]
Mingzhu Ye[1]
Xinggang Yang[1]
Weisan Pan[1]

[1]Department of Pharmaceutics, School of Pharmacy, Shenyang Pharmaceutical University, Shenyang 110016, People's Republic of China; [2]Key Laboratory of Ministry of Education for TCM Viscera-State Theory and Applications, Liaoning University of Traditional Chinese Medicine, Shenyang 110016, People's Republic of China

Background: The objective of this study was to develop a more bio-available and safe nanosuspension of meloxicam (MX), which could dramatically improve inflammation targeting.
Methods and results: MX-loaded bovine serum albumin (BSA) nanosuspensions were prepared using acid–base neutralization in aqueous solution and the prepared nanosuspensions were characterized. The results obtained showed that the prepared nanosuspensions had a narrow size distribution with a mean particle size of 78.67±0.22 nm, a polydispersity index of 0.133±0.01, and a zeta potential of −11.87±0.91 mV. The prepared MX nanosuspensions were spherically wrapped by BSA with a smooth surface as shown by transmission electron microscopy. Stability studies showed that the nanosuspensions were physically stable at 4°C with a shelf life of at least 6 months. In the in vitro dissolution test, the MX-loaded BSA nanosuspension (MX-BSA-NS) exhibited sustained release. In addition, an in vivo pharmacokinetic study in rats following intravenous injection showed that the half-life ($t_{1/2}$), mean residence time (MRT), and area under the concentration–time curve ($AUC_{0-\infty}$) of MX-BSA-NS was increased by 169.83%, 150.13%, and 148.80%, respectively, in comparison with MX conventional solution (MX solution). Furthermore, results from inflammation targeting studies showed that the concentration of MX increased significantly in inflamed tissues but was reduced in normal tissues compared with the MX solution group after injection of MX-BSA-NS.
Conclusion: The prepared MX-BSA-NS significantly increased the inflammation-targeting properties and bioavailability of MX, suggesting its potential as a promising formulation for the targeted drug delivery of MX in future clinical applications.
Keywords: nanosuspensions, inflammation targeting, BSA, meloxicam, acid–base neutralization

Introduction

Meloxicam (MX) is a potent COX-2 inhibitor of the enolic acid class of oxicam derivatives with anti-inflammatory, analgesic, and antipyretic effects.[1,2] Compared with other earlier nonsteroidal anti-inflammatory drugs, MX causes less irritation to the gastrointestinal tract and has a superior safety profile.[3–6] Unfortunately, MX has an extremely low aqueous solubility at physiological pH, which reduces its bioavailability and hinders its clinical application.[7–9] Several attempts have been made to improve the bioavailability and therapeutic effect of MX. Nanonization strategies have been shown to be very promising approaches to improve the dissolution.[10,11] The use of nanosuspensions is one attractive nanoscience approach for the intravenous (iv) administration of MX, and the reduced particle size and large specific surface area of nanosuspensions lead to an increase in the dissolution and saturation solubility of loaded drugs.[12–14] Compared with some other nanostructured carriers such as micelles,[15,16]

Correspondence: Weisan Pan; Xinggang Yang
Department of Pharmaceutics, School of Pharmacy, Shenyang Pharmaceutical University, 103 Wenhua Road, Shenyang 110016, People's Republic of China
Tel +86 4352 0533
Email pppwwwsss@163.com; yangxg123@163.com

submit your manuscript | www.dovepress.com
Dovepress
http://dx.doi.org/10.2147/IJN.S160714

gold nanoparticles,[17,18] and nanoemulsion,[19] nanosuspensions have a number of advantages including reduced toxicity, simple formulation, and established preparation technology. When intravenously administered, nanosuspensions can alter the drug biodistribution and increase drug accumulation in tumors and inflamed tissues by an enhanced permeability and retention (EPR) effect.[20–24]

Nevertheless, due to Ostwald ripening, nanosuspensions aggregate to reduce the system's Gibbs free energy, and, as a result, this behavior makes the nanosystem become unstable. To stabilize nanosystems, stabilizers are commonly used to prevent aggregation and agglomeration of the drug particles. However, most conventionally used stabilizers may cause potential toxicity of the nanosuspension. Therefore, developing a suitable stabilizer with a low toxicity and superior stabilization efficiency is a very important aspect of nanotechnology. Recently, BSA has been commonly used as a suitable carrier and stabilizer for drug delivery systems due to its superior advantages, such as a lack of immunogenicity, toxicity, and good biodegradability.[25–27] In addition, BSA exhibits easy accumulation and good uptake in inflamed tissues,[28] and it has been investigated in various drug delivery systems, such as nanoparticles,[29,30] microspheres,[31,32] conjugates,[33,34] and nanosuspensions.[35] Currently, BSA is widely used as an excellent stabilizer instead of other organic stabilizers with potential toxicity, such as sodium dodecyl sulfate (SDS), Poloxamer 188, and Poloxamer 407.[22,30,36,37]

In general, two basic methods are used to obtain drug nanosuspensions. One is the chemical precipitation method (bottom-up) and the other is the disintegration process (top-down).[38] In chemical precipitation, antisolvent precipitation is a leading method for manufacturing drug nanoparticles by mixing the organic solvents containing a water-insoluble drug with an aqueous solution.[39] However, the organic solvent residue remaining in the final product is a problem, and the use of organic solvents may not be desirable because they may cause toxicity. Recently, increasing attention has focused on acid–base neutralization reaction, a simpler manufacturing strategy with highly practical potential.

Although many hydrophobic drugs cannot dissolve in aqueous solution, they are more soluble in strong basic or acidic solutions such as sodium hydroxide. Therefore, based on the property mentioned earlier, an acid–base neutralization reaction has an enormous potential for preparing nanosuspensions and can be used in a number of industrial pharmaceutical applications.[40,41]

In this study, we prepared a novel MX nanosuspension through the bottom-up approach by using an acid–base neutralization reaction. We used BSA combined with Tween-80 to increase the stability of the MX nanosuspension without using excess toxic stabilizer, which differs quite dramatically from previous commercially available MX formulations. The prepared nanosuspensions were subsequently dried by freeze drying, and in vitro properties, as well as in vivo bioavailability, of the MX-BSA-NS were investigated and compared with those of MX conventional solution (MX solution). The physiochemical properties of the dried MX nanosuspensions were characterized by dissolution studies, particle size analysis, and transmission electron microscopy (TEM). A cell viability assay was used to evaluate the cytotoxicity of MX to murine RAW264.7. Furthermore, to prove that the prepared nanosuspension has better bioavailability and targeting properties, a pharmacokinetic study of MX-BSA-NS and MX solution was carried out in rabbits and the target effects were evaluated in rats.

Materials and methods

Materials

MX (CAS no 71125-38-7) was obtained from Kangya Pharmaceutical Co, Ltd (Ningxia, People's Republic of China). BSA was obtained from Roche Pharmaceutical Co, Ltd (Shanghai, People's Republic of China). Tween-80 (CAS no 9005-65-6) was obtained from Jiangbei Chemical Co. (Wuhan, People's Republic of China). Lornoxicam was obtained from Linhai Xinghua Chemical Co, Ltd (Linhai, People's Republic of China). All the chemicals used in this study were of analytical or high-performance liquid chromatography (HPLC) grade. 3-(4,5-Dimethylthiazol-2-yl)-2,5-diphenyl-tetrazoliumbromide (MTT; 98%) was obtained from Alfa Aesar (People's Republic of China) Chemical Co, Ltd (Shanghai, People's Republic of China), and fetal bovine serum (FBS) was obtained from Sijiqing Co, Ltd (Hangzhou, People's Republic of China). Carrageenan was obtained from HWRK Chemical Co, Ltd (Beijing, People's Republic of China). DMEM was obtained from Hyclone Co, Ltd (Thermo Fisher Scientific, Waltham, MA, USA).

Animals

New Zealand white albino rabbits (weighing 1.5–2.0 kg) and Sprague Dawley rats (weighing 180–220 g) were obtained from Shenyang Pharmaceutical University Animal Centre (Shenyang, People's Republic of China). All the animal experiments were carried out in compliance with the guidelines for the Care and Use of Laboratory Animals of Shenyang Pharmaceutical University. Ethical approval was obtained for the use of animals in this study from the review

board for the Care and Use of Cells/Laboratory Animals of Shenyang Pharmaceutical University. All animals were housed under standard conditions (a temperature of 25°C and a relative humidity of 55°C).

Optimization of preparation of MX-BSA-NS

Prior to optimization of the formulation, the pH of the reaction system was evaluated, and various kinds and contents of cryoprotectants were screened. The key parameters were defined in a series of preliminary experiments. The content of Tween-80, MX, and the weight ratio of MX to BSA (MX:BSA, w/w) were considered as the critical parameters in the preparation process with an effect on particle size, and the particle size after 24 h and the stability time of the nanosuspensions were used as an index. The single-factor method was used to evaluate and optimize the selected parameters during the experiment.

The content of Tween-80 ranged from 0.1% to 0.4%, while the content of MX ranged from 2.5 to 7.5 mg mL^{-1}, and the weight ratio of MX to BSA was set from 1:1 to 1:5. All the levels are shown in Table S1.

Preparation of MX-BSA-NS and MX solution

MX-BSA-NS was prepared based on the pH-dependent solubility of MX. Briefly, 0.3 g of Tween-80 was dissolved in 20 mL hydrochloric acid solution (0.1 M), whereas 0.5 g of MX was dissolved in 20 mL sodium hydroxide solution (0.1 M), and 2.5 g of BSA and 5 g of mannitol was added to 40 mL of distilled water. Then, the sodium hydroxide solution with MX was slowly added to the hydrochloric acid solution under moderate stirring at 4°C–8°C. After the sodium hydroxide solution was completely dispersed in acid solution, more sodium hydroxide solution was added to adjust the pH to 5.8. Next, distilled water containing BSA and mannitol was added dropwise with sustained stirring at 4°C–8°C and the reaction continued for 12 h. Then, distilled water was added to produce the desired nanosuspension. Finally, the obtained suspension was transferred to 1.5 mL vials and frozen at −74°C in a freezer for 8 h. The resultant nanosuspension dispersion was freeze dried at −25°C for 12 h and then kept at 25°C for 3 h to obtain nanosuspension powders. The MX nanosuspensions without BSA were prepared according to the above procedure except that BSA was not added.

The MX solution was prepared as follows: 10 mg MX was dissolved in 1 mL of dimethylacetamide by sonication. Then, PBS (pH=7.2) was added and the resultant solution was passed through a 0.22 μm microfiltration membrane to obtain 1.0 mg mL^{-1} MX solution.

Characterization of MX-BSA-NS

Reconstitution of dried MX-BSA-NS

Redispersed MX-BSA-NS was prepared as follows: about 12.45 mg (weight of the lyophilized sample in a single vial) MX-BSA-NS freeze-dried powder was dispersed in a single vial with 1.5 mL of purified water to obtain 5.0 mg mL^{-1} of redispersed MX-BSA-NS. Then, the appearances of raw MX-BSA-NS (MX-BSA-NS before lyophilization), MX-BSA-NS freeze-dried powder, and redispersed MX-BSA-NS were recorded photographically.

Particle size and zeta potential

The particle size and zeta potential of MX-BSA-NS before lyophilization and after lyophilization were separately measured by dynamic light scattering (DLS) using a Zetasizer Nano (Malvern Instruments, Malvern, UK) at 25°C. Prior to measurement, the lyophilized MX-BSA-NS powder was reconstituted as described in the "Reconstitution of dried MX-BSA-NS" section. The samples were then diluted with distilled water, and 1.5 mL of redispersed MX-BSA-NS (5.0 mg mL^{-1}) and 1.5 mL of raw MX-BSA-NS (5.0 mg mL^{-1}) were used as samples. All measurements were repeated three times, and the average value of each was used.

Fourier transform infrared (FTIR)

In order to identify whether the BSA was conjugated to the nanoparticle, FTIR was performed using an FTIR spectrometer (IFS55; BrukerOptik GmbH, Ettlingen, Germany). The spectra were recorded in the wavenumber range of 500–4,000 cm^{-1} with a resolution of 4 cm^{-1}. The samples (1%, w/w) were mixed well with KBr and further pressed into pellets.

X-ray powder diffraction (XRD)

The physical state of samples (MX, dried MX nanosuspensions, BSA, mannitol, and physical mixture) was verified by XRD. For this, a physical mixture was obtained by mixing MX, BSA, and mannitol in a proportion of 1:5:10 according to the formulation. Each sample weighed 0.1 g, and the XRD patterns were recorded between 10° and 90° using an X-ray diffractometer (D8 Advance Diffractometer; BrukerOptik GmbH). A Cu radiation source was used as the anode material, the step size (2θ) was 0.02°, and the measurement temperature was 25°C.

TEM

The morphology of MX-BSA-NS was observed using a TEM (JEM-1200EX; JEOL, Tokyo, Japan). The samples were diluted with distilled water, then placed on a carbon-coated copper grid, and dried at ambient temperature. Prior to observation, the samples were negatively stained with 2.0% (w/v) phosphotungstic acid.

In vitro release

In vitro release of MX-BSA-NS was carried out in a dissolution testing apparatus by dialysis according to the *Chinese Pharmacopoeia* dissolution procedure. Samples of MX-BSA-NS were obtained by dissolving 12.45 mg of lyophilized powder in 1.5 mL of distilled water with gentle shaking. Then, the MX-BSA-NS and MX solution were injected into the dialysis bag and this was dialyzed against 500 mL of PBS (pH=7.4) at 37°C±0.5°C with a paddle speed of 50 rpm. At predetermined intervals (2 min, 5 min, 10 min, 15 min, 20 min, 30 min, 1 h, 1.5 h, 2 h, 3 h, 4 h, and 6 h), samples (1.0 mL) were removed and replaced with an equal volume of temperature-equilibrated fresh dissolution medium. All samples were passed through a 0.45-μm filter, and the initial filtrate was discarded. Then, the remainder was collected for HPLC analysis. Dissolution studies were performed in triplicate.

The HPLC analysis was performed using a Shimadzu LC-10A system (Shimadzu, Kyoto, Japan) consisting of an LC-10AT HPLC pump and an SPD-10A UV-VIS detector with a Diamonsil C18 column (5 μm, 200 × 4.60 mm). The detection wavelength was set at 254 nm, the column temperature was maintained at 30°C, and the mobile phase consisted of methanol, 0.1 M ammonium acetate solution (65:35, v/v) at a flow rate of 1.0 mL min^{-1}, and the sample injection volume was 20 μL. The assay was linear (r^2=0.9999) over the concentration range of 5.0–1000.0 ng mL^{-1}.

Stability studies

The physical and chemical stabilities of the lyophilized MX-BSA-NS were investigated by storing samples at 4°C for 6 months. Aliquots of MX-BSA-NS were withdrawn at 0, 1, 2, 3, and 6 months, and their appearance, content, particle size distribution, and zeta potential were determined. Each sample was analyzed in triplicate.

Cell culture

The cell experiments were carried out in compliance with the guidelines for the Care and Use of Cells of Shenyang Pharmaceutical University. The murine RAW264.7 cell line was obtained from Fenghui BioTECH Co, Ltd (Changsha, Hunan, People's Republic of China). The cells were cultured in DMEM-containing heat-inactivated 10% FBS, 100 U mL^{-1} of penicillin and 100 μg mL^{-1} of streptomycin at 5% CO_2 and at 37°C in a humidified atmosphere. The medium was changed every 2 days.

Cell viability assay

The MTT colorimetric method was used to determine the cell viability. RAW264.7 cells were seeded into 96-well plates (1×10^5 cells per well) and incubated with different concentrations of samples (0, 10, 20, 40, 60, 80, 100, and 120 μg mL^{-1}) for 24 h. Then, MTT (0.5 mg mL^{-1}) was added to each well and the solutions were further incubated for another 4 h under 5% CO_2 at 37°C. The supernatant was then discarded, and the generated formazan product was dissolved in dimethyl sulfoxide. The absorbance at 570 nm was measured using a microplate reader (MK3; Thermo Fisher Scientific). All measurements were performed in triplicate.

$$\text{Cell viability (\%)} = (A_2 - A_0)/(A_1 - A_0) \times 100$$

where A_1 is the absorbance of the untreated group, A_2 is the absorbance of samples group, respectively, and A_0 is the absorbance of the medium. The half maximal inhibitory concentration (IC_{50}) values were calculated by the SPSS 17.0 software.

Pharmacokinetic studies

The pharmacokinetics of MX was investigated in New Zealand white albino rabbits. Twelve rabbits (six males and six females) were randomly divided into two groups of six animals each. After the rabbits were fasted for 12 h, MX-BSA-NS and MX solution (0.7 mg kg^{-1} body weight expressed as MX equivalents) were given to the rabbits in the two groups via an iv injection. After administration, 1.5 mL of blood samples was collected from the ear vein at 0.1, 0.5, 1, 2, 4, 8, 12, 24, 48, 72, and 96 h. The blood samples were transferred to heparinized tubes and immediately centrifuged at 4,000 rpm for 10 min, and the supernatant was stored at −20°C until required for extraction and analysis.

The plasma samples were treated as follows: plasma samples were left to equilibrate to room temperature before HPLC analysis. Then, 500 μL of each plasma sample was transferred to 10 mL polyethylene tubes and 50 μL of Lornoxicam solution (20 μg mL^{-1}) was added as an internal standard, followed by vortex mixing for 30 s. Then, 0.1 M

HCl solution was added, followed by vortexing for 2 min. Next, 4 mL of a mixture (hexane:dichloromethane:isopropanol=20:10:1) was added, and the samples were vortexed for an additional 5 min, followed by centrifugation at 4,000 rpm for 10 min. The supernatants were evaporated at 40°C under a gentle stream of nitrogen, and the dried samples were reconstituted in 100 µL of mobile phase and then vortexed for 2 min. After centrifugation at 4,000 rpm for 5 min, 20 µL of supernatant was withdrawn and used for HPLC analysis.

Inflammation targeting studies and paw edema assay

Incisional surgery was performed as previously described.[42] Typically, 24 male Sprague Dawley rats were randomly divided into two groups of 12 animals each and each group was further divided into four time groups (0.25, 0.5, 1, and 2 h), each containing three animals. Rats were anesthetized with diethyl ether, and the plantar surface of the left hind paw was prepared under sterile conditions. A 1 cm longitudinal incision was made through skin and fascia of the plantar aspect of the left hind paw, starting 0.5 cm from the proximal edge of the heel and extending toward the toes. The plantaris muscle was then elevated, and an incision was made longitudinally, keeping the muscle origin and insertion site intact. After bleeding was stopped by gentle pressure, the skin was sutured with two single stitches using 5–0 nylon. The rats were allowed to recover for 15 min, and then MX-BSA-NS and MX solution, at an equivalent dose of 25 mg kg^{-1}, were given to the rats via a tail vein injection. After administration, rats in the four time groups were sacrificed at predetermined intervals and the plantaris muscles of both left and right hind paws were harvested and immediately washed with normal saline.

Accurately weighed tissue samples were homogenized with normal saline (0.1 g mL^{-1}) in an ice bath using a homogenizer. Then, 50 µL of lornoxicam solution (20 µg mL^{-1}) was added to 1 µL of tissue homogenates followed by vortexing for 30 s and the subsequent operations were the same as described in the "Pharmacokinetic studies" section. The prepared samples were then analyzed by HPLC.

Another 18 male Sprague Dawley rats were randomly divided into three groups of six animals each (control group, MX solution group, and MX-BSA-NS group). All the rat models were performed as follows: 100 µL of 1% (w/v) carrageenan suspension was injected into the subplantar of the rat right hind paw.[43] Thirty minutes prior to the injection of carrageenan, the control group was injected with saline and the MX solution group and MX-BSA-NS group were injected with MX solution and MX-BSA-NS (25 mg kg^{-1}), respectively. The paw volumes (mL) were measured before and after injection of carrageenan (1, 2, 4, and 6 h) by using a toe volume measuring instrument (PV-200; Techman software Co, Ltd, Chengdu, People's Republic of China). The edema rate was used as an index to evaluate paw edema: edema rate (%)=(paw volume after modeling–paw volume before modeling)/paw volume before injection×100.

Statistical analyses

Data analysis was performed using the DAS 2.0 and SPSS 17.0 software and expressed as the mean value±SD. Statistical analyses were conducted by analysis of variance. For all data, a P value of <0.05 was considered as being statistically significant.

Results and discussion

Optimization of preparation of MX-BSA-NS

First, according to the results of the solubility measurements (Table S2), MX was most soluble in 0.1 M sodium hydroxide solution; hence, 0.1 M sodium hydroxide solution was selected as the solution to dissolve MX. After several experiments, it was found that when the concentration of acid and alkali was equal, the pH value could be adjusted conveniently and accurately. Therefore, 0.1 M hydrochloric acid solution was selected as the solution to dissolve the stabilizer. Subsequently, we carried out a screening of cryoprotectants. As seen in Tables S3 and S4 and Figure S1, if mannitol was used as a cryoprotectant, when the concentration was 5% (w/v), the product was found to have a smooth and compact appearance and the nanosuspension after reconstitution was translucent and was hardly changed compared with the other products. Thus, 5% (w/v) mannitol was chosen as the cryoprotectant in the formulation.

Finally, single-factor experiments were used to determine the optimal parameters. In each experiment, one of the variables was changed to assess their influence on particle size and the stability time of the nanosuspension. The results of the particle size and stability time for all the experiments are shown in Table S1. As shown in Table S1, with an increase in the content of Tween-80, the particle size of the nanosuspension decreased, while the stability increased first and then decreased. Based on the experimental data, we chose 0.3% (w/v) as the optimum level of Tween-80. Also, when the weight ratio of MX to BSA was 1:5, the nanosuspension had a smaller particle size and better stability. As can be seen from the results in the table, as the content of MX increased, the particle size of MX-BSA-NS decreased but the particle

aggregation accelerated, which reduced the stability. When the content of MX was 5 mg mL^{-1}, the particle size and stability met the requirements of the formulation.

To sum up, the optimal formulation was as follows: the content of Tween-80 was 0.3% (w/v), the weight ratio of MX to BSA was 1:5, and the content of MX was 5 mg mL^{-1}.

Preparation of MX-BSA-NS and MX solution

According to our studies, MX displayed an extremely low solubility of ~7.9 μg mL^{-1} in water. At pH 5.8, the solubility was 0.0183 mg mL^{-1}. Within a certain range, the solubility of MX increased significantly as the pH of the solution increased and reached a maximum of ~32.48 mg mL^{-1} when dissolved in 0.1 M NaOH solution. However, if the pH of the solution continued to rise, the solubility decreased instead. Hence, acid–base neutralization can be used to prepare nanosuspensions on account of the pH-dependent solubility of MX. A certain amount of MX was dissolved in 0.1 M NaOH solution and then added drop wise to the acid solution. With an increase in acidity, the solubility of MX dissolved in NaOH solution fell abruptly so that the MX molecules quickly grew into cores and further precipitated into drug nanoparticles. The nanoparticles obtained by this method exhibited a smaller particle size and were further stabilized by the presence of BSA. BSA was adsorbed to the surface of the particles to provide sufficient steric stability and electrostatic repulsion, making a great contribution to maintain the small particle size.[44] The MX-BSA-NS can remain stable for >15 days (Figure S2), but the MX nanosuspension without BSA coating precipitated after 24 h due to the protective coating of BSA (Figure S2). Among various stabilizers, Tween-80 showed the best properties. When added to the nanosuspension system, Tween-80 adhered to the surface of the drug particles and formed a protective layer to reduce the solid–liquid interfacial tension. Thus, Tween-80 hindered particle aggregation, which plays an important role in inhibiting the growth of MX nanoparticles.[45]

Characterization of MX-BSA-NS

Reconstitution of dried MX-BSA-NS

The redispersibility study was carried out to confirm the physical stability of the prepared nanosuspension after lyophilization. In general, BSA itself can be used as a freeze-dried protective agent. Nonetheless, the freeze-dried products have a large particle size in the case of BSA as the only protective agent. Therefore, based on these results, 5% mannitol had a significant advantage in particle size protection and the shortest reconstitution time. In this study, BSA was combined with mannitol to provide excellent protection for the nanosuspension during the freeze-drying process. As shown in Figure 1, the freeze-dried MX-BSA-NS was a loose, light yellow powder with a smooth surface and was well dispersed. Furthermore, there was no distinct change in appearances between MX-BSA-NS before lyophilization and after redispersion. Thus, it can be inferred that the MX-BSA-NS was stable after lyophilization. However, further studies are required to confirm this.

Particle size, zeta potential, and morphology

The particle size and polydispersity index (PI) are the most important characteristics of nanosuspensions. The following characteristics of nanosuspensions were closely related to the particle size: 1) physical stability; 2) drug saturation solubility; 3) bioavailability; and 4) dissolution rate.

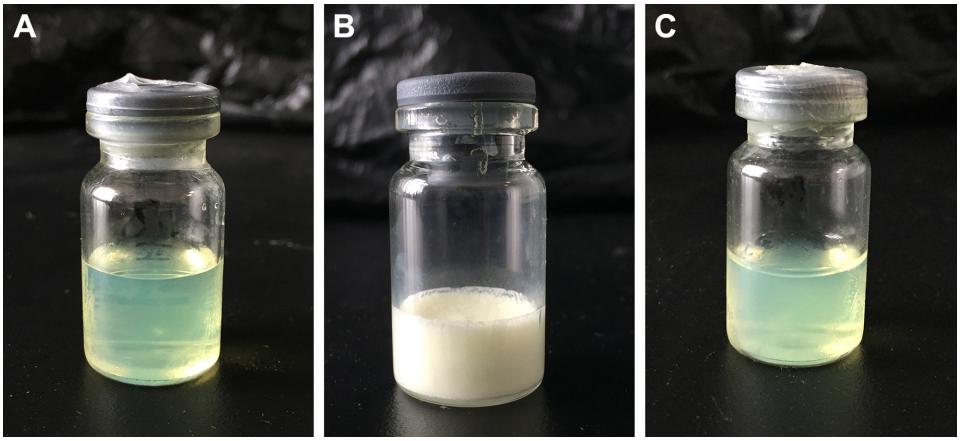

Figure 1 Appearance of MX-BSA-NS before lyophilization (**A**), after lyophilization (**B**), and after redispersion (**C**).
Abbreviations: BSA, bovine serum albumin; MX, meloxicam; NS, nanosuspension.

Decreasing the particle size produces a considerable increase in the particle surface area, which increases the drug solubility in aqueous solutions, and this can be explained by the Whitney equation:

$$dM/dt = DA(C_s - C_t)/h$$

where dM/dt is the dissolution velocity, D represents the diffusion coefficient, A is the surface area, h is the diffusion distance, C_s is the saturation solubility, and C_t is the bulk concentration. Thus, a reduction in drug particle size to the nanoscale leads to an increased dissolution rate and can further improve the bioavailability of the drug particles.

Three batches of MX-BSA-NS prepared with the optimal formulation and processing parameters were used in this study. The mean diameter, PI, and zeta potential were 78.67±0.22 nm, 0.133±0.01, and −11.87±0.91 mV, respectively. After lyophilization, these values changed to 90.36±0.58 nm, 0.147±0.08, and –8.8±0.56 mV, respectively. As shown in Figure 2, the PI was 0.1–0.3, indicating a narrow particle size distribution, which supports the good physical stability of nanosuspensions.[46,47] Since the zeta potential was comparatively low, the nanosuspensions did not tend to agglomerate. This may be because the drug particles were coated with BSA. Moreover, the Tween-80 adhered to the particle surface to form polymer layers. BSA and Tween-80 may provide marked steric stabilization. When combined with steric stabilization, electrostatic stabilization could be sufficient to prevent drug particles from undergoing aggregation and precipitation.

A TEM study showed that the homogeneous nanoparticles did not adhered to each other (Figure 3). The TEM image showed that MX-BSA-NS was almost spherical with a smooth surface. Most of the particles were ~100 nm in size, which almost in agreement with the DLS results. Moreover, BSA wrapped on the surface of nanoparticles could be observed clearly.

FTIR analysis and XRD

The obtained FTIR spectra well supported the conjugation of BSA on the surface of nanoparticles. As shown in Figure 4, BSA spectra have two characteristic vibration bands at 1,632 cm^{-1} (amide I) assigned to the stretching vibration of –C=O and 1,534 cm^{-1} (amide II) assigned to the C–N stretching vibration and N–H bending vibration. Moreover, from MX-BSA-NS spectra, dominant band at ~1,632 and 1,547 cm^{-1} can be observed, which cannot be seen in the spectra of mixture. The migration of peak positions at 1,654 cm^{-1}

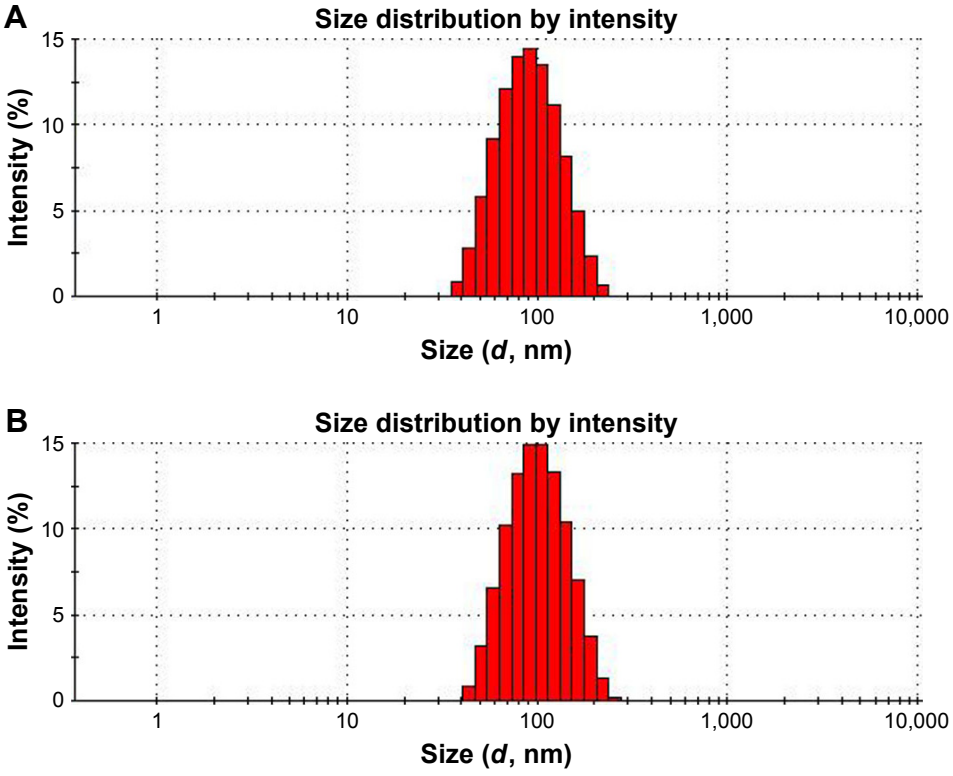

Figure 2 Particle size and distribution of MX-BSA-NS before lyophilization (**A**) and after lyophilization (**B**).
Abbreviations: BSA, bovine serum albumin; MX, meloxicam; NS, nanosuspension.

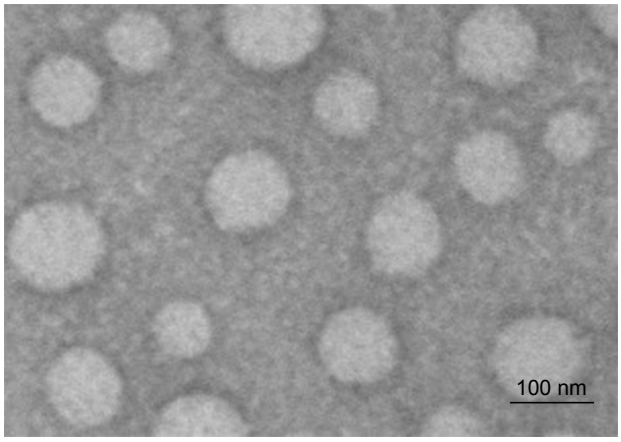

Figure 3 Transmission electron microscopy morphology of MX-BSA-NS.
Abbreviations: BSA, bovine serum albumin; MX, meloxicam; NS, nanosuspension.

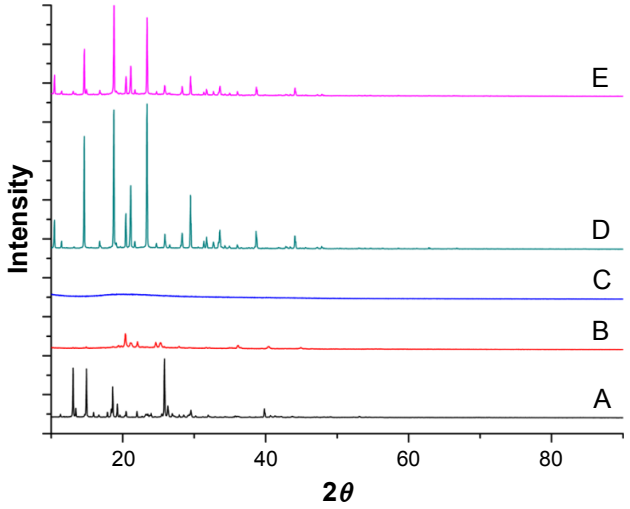

Figure 5 X-ray powder diffraction patterns of (A) raw MX, (B) dried MX nanosuspensions, (C) BSA, (D) mannitol, and (E) physical mixture.
Abbreviations: BSA, bovine serum albumin; MX, meloxicam.

and the reduction of the peak intensity at 1,547 cm^{-1} may be attributed to changes in the secondary structure of BSA. So, it can be concluded that BSA had been conjugated to the nanoparticles.

XRD was performed to assess the physical state of MX in the dried nanosuspensions. The patterns of the bulk MX, MX nanosuspensions, BSA, mannitol, and the physical mixture are illustrated in Figure 5. As shown in Figure 5, raw MX exhibited sharp, distinctive peaks at 2θ values 13.4, 14.9, 18.6, and 25.8°, whereas BSA exhibited a halo pattern, indicating its amorphous structure. In addition, several sharp peaks were observed in mannitol, showing that the mannitol used in the formulation was polymorphic As for the MX nanosuspensions, MX and mannitol did not show any peaks, suggesting that they were present in an amorphous state in the dried nanosuspensions. This may be because BSA and Tween-80 were coated on the surface of MX during the period of storage, resulting in repulsion between the precipitated nanoparticles, which hindered the formation of the crystal form, eventually leading to the MX in the formulation having an amorphous form. The MX in the nanosuspension is amorphous, which could increase the apparent solubility and the dissolution rate.[48]

In vitro release

Dissolution studies of MX solution and MX-BSA-NS were carried out, and the results are shown in Figure 6. For the MX solution, ~100% of the drug was released within 1 h,

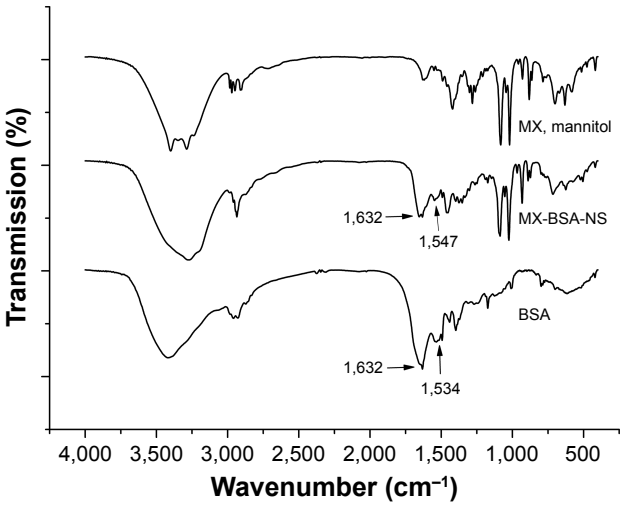

Figure 4 FTIR spectrum of BSA, MX-BSA-NS, and MX mixture (MX, mannitol).
Abbreviations: BSA, bovine serum albumin; FTIR, Fourier transform infrared; MX, meloxicam; NS, nanosuspension.

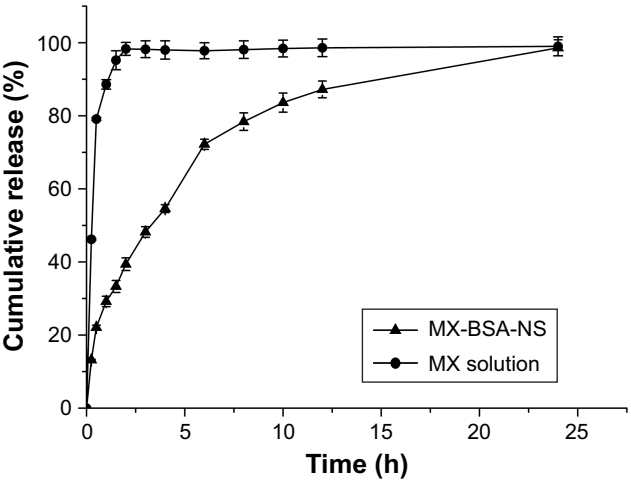

Figure 6 In vitro release profile of MX from different vehicles at pH 7.4.
Note: The data are shown as mean ± standard deviation (SD).
Abbreviations: BSA, bovine serum albumin; MX, meloxicam; NS, nanosuspension.

Table 1 Stability of MX-BSA-NS after lyophilization under 4°C

Batches	Time (months)	Appearance	Content (%)	PS (nm)	PI	Zeta potential (mV)
20160826	0	Yellow bulk powder	99.7	90.43	0.155	–8.7
	1	Yellow bulk powder	100.2	91.37	0.136	–8.8
	2	Yellow bulk powder	99.5	91.98	0.147	–8.5
	3	Yellow bulk powder	98.9	92.29	0.158	–9.0
	6	Yellow bulk powder	98.6	92.47	0.154	–8.7
20160827	0	Yellow bulk powder	99.2	89.75	0.147	–8.9
	1	Yellow bulk powder	98.9	90.12	0.156	–8.8
	2	Yellow bulk powder	98.7	90.55	0.149	–8.6
	3	Yellow bulk powder	99.2	91.18	0.153	–8.3
	6	Yellow bulk powder	98.3	90.82	0.166	–8.5
20160828	0	Yellow bulk powder	99.4	90.91	0.139	–8.5
	1	Yellow bulk powder	99.1	90.49	0.148	–9.2
	2	Yellow bulk powder	98.9	91.38	0.154	–8.8
	3	Yellow bulk powder	99.1	92.74	0.145	–8.4
	6	Yellow bulk powder	98.2	91.89	0.143	–8.7

Abbreviations: BSA, bovine serum albumin; MX, meloxicam; NS, nanosuspension; PI, polydispersity index; PS, particle size.

whereas MX-BSA-NS showed only ~40% release at 2 h and only 50% of the applied MX was released at 3 h. In other words, MX-BSA-NS was released significantly more slowly than the MX solution group. Compared with MX solution, MX-BSA-NS exhibited sustained release, which was probably due to the coating of BSA-hindered drug dissolution from the drug particle surfaces. BSA formed a protective shell on the drug particle surface to provide a steric stabilization effect, which also prevented release of the drug. This may allow more accumulation of nanoparticles in inflammatory tissues during the long-term circulation. This would help the drug nanosuspension be more effective while reducing its side effects.

Stability studies

From the data shown in Table 1, we can conclude that the lyophilized MX-BSA-NS exhibits no obvious change in appearance after storage at 4°C for 6 months, and only a slight increase in particle size, PI, and zeta potential was observed. Almost no change in the drug concentration was observed after storing the nanosuspensions at the same temperature for the same time, indicating that no chemical degradation of MX occurred after long storage. The particle size was slightly increased, and this could be explained by the fact that there was a large surface energy between the nanoparticles. The aggregation of nanoparticles can reduce the surface energy, which makes the system more stable. Therefore, to improve the thermodynamic stability, the nanoparticles showed a tendency to aggregate, resulting in a slight increase in the particle size.[49] The results reported earlier indicate that the optimized nanosuspension formulation was physically and chemically stable with a shelf life of at least 6 months, which might be due to the presence of BSA. Moreover, the Tween-80 used in the formulation adequately covers the surface of the particles, which could provide sufficient steric repulsion between particles.[50]

Cell viability assay

Cell viability was assessed using an MTT assay, and the results are given in Figure 7. From Figure 7, we can observe that with the increasing of MX concentrations,

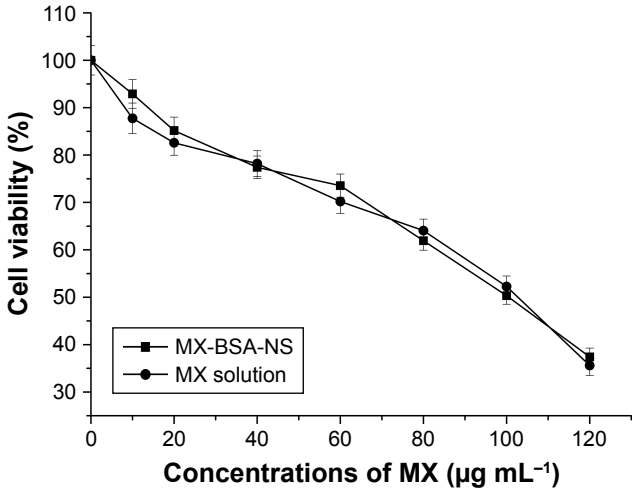

Figure 7 Cell viability of RAW264.7 murine macrophage cells assessed by MTT assay after exposure to different concentrations of MX (0–120 μg mL^{-1}) in different vehicles for 24 h.

Note: The data are shown as mean±SD of three independent experiments.

Abbreviations: BSA, bovine serum albumin; MTT, 3-(4,5-dimethylthiazol-2-yl)-2,5-diphenyl-tetrazoliumbromide; MX, meloxicam; NS, nanosuspension.

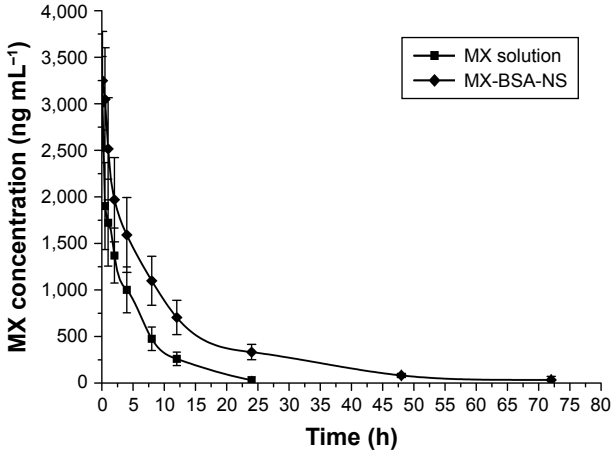

Figure 8 Mean blood concentration–time curve of MX in rabbits after intravenous administration of MX solution and MX-BSA-NS.
Note: Each value represents the mean±SD, n=6.
Abbreviations: BSA, bovine serum albumin; MX, meloxicam; NS, nanosuspension.

the cell viability of RAW264.7 decreased in a dose-dependent manner. In addition, MX-BSA-NS and MX solution have similar curve and there was no marked difference between two groups ($P>0.05$), suggesting that both samples released a similar amount of MX after 24 h. Furthermore, MX-BSA-NS and MX solution have approximate IC_{50} values 103.94 and 109.124 μg mL^{-1}, respectively.

Pharmacokinetic studies

Pharmacokinetic studies were used to determine whether a nanosuspension is able to improve the bioavailability of MX. The average plasma concentration–time curves of the MX-BSA-NS and MX solution are shown in Figure 8, and the pharmacokinetic parameters are given in Table 2. These parameters show that there are clear differences between MX-BSA-NS and MX solution. The half-life ($t_{1/2}$) of the nanosuspension was 11.600 h, which was significantly prolonged in comparison with the $t_{1/2}$ of the MX solution. Moreover, the MX-BSA-NS had higher mean residence time (MRT) (2.5-fold higher), area under the concentration–time curve ($AUC_{0-\infty}$) (2.49-fold higher), and lower clearance (Cl) (61.67% lower) than the MX solution, showing that the nanosuspension exhibited a sustained release. This phenomenon might be caused by the dissolution pattern of MX-BSA-NS. After iv administration, the drug in MX-BSA-NS was released slowly into the blood circulation due to the blockage of BSA on the particle surface, which led to a prolonged residence time. As a result, the bioavailability of MX was dramatically increased.

Inflammatory tissue targeting studies and paw edema assay

To gain a deeper insight into the in vivo behavior of MX-BSA-NS, incisional surgery in rats was conducted and HPLC was proved to be an effective method for determining the MX concentrations in inflammatory tissue. The method recovery, the extraction recovery of MX from rat tissues, the relative standard deviations, the accuracy, and linearity intraday and interday satisfied the requirements of analysis for biological detection.

After injection of MX-BSA-NS and MX solution, the concentrations of MX in left and right paws are shown in Figure 9. As shown in Figure 9, after the administration of MX solution, the concentration of MX in the surgical side was higher than in the nonsurgical side, indicating that the drug itself has a certain degree of inflammation targeting. This may be because the MX has a relatively high plasma albumin binding rate, and albumin possesses inherent targeting to the inflammatory site. The expansion of spaces between vascular endothelial cells due to inflammatory lesions allowed the drug nanoparticles to easily pass through the damaged vascular endothelial cells into the inflammatory tissues.[51] In addition, as a result of lymphatic drainage system defects, the drug can accumulate in the inflammatory tissues for a long period instead of being removed quickly. Also, compared with the MX solution group, the concentration of MX in the surgical side after administration of MX-BSA-NS was clearly higher. This may be because BSA wrapped on the surface of the drug nanoparticles exhibited natural targeting of inflammatory tissues, making it easier for the drug nanoparticles to reach the operatively incised tissues. Thus, nanoparticles could preferentially gather on the surgical side and accumulate over time, displaying superior targeting effects.

Table 2 Main pharmacokinetic parameters of MX solution and MX-BSA-NS following intravenous injection in rabbits (mean±SD, n=6)

Preparation	$t_{1/2}$ (h)	$AUC_{0-\infty}$ (ng L^{-1} h)	Cl (L h^{-1} kg^{-1})	MRT (h)
MX solution	4.299±0.682	12,351.267±3,038.82	0.06±0.015	5.683±0.666
MX-BSA-NS	11.6±2.16	30,730.213±3,741.436	0.023±0.003	14.215±3.144

Note: $t_{1/2}$, half-life.
Abbreviations: $AUC_{0-\infty}$, area under the concentration–time curve; Cl, clearance; MRT, mean residence time; BSA, bovine serum albumin; MX, meloxicam; NS, nanosuspension.

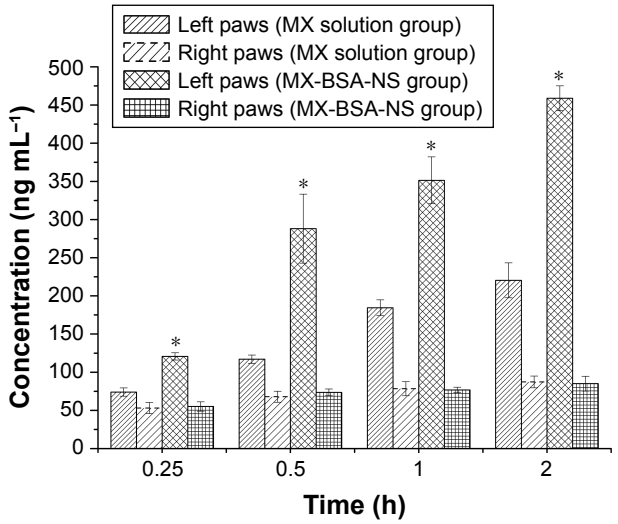

Figure 9 Mean concentration of MX in rats' paws after intravenous administration of MX solution and MX-BSA-NS.
Note: *$P<0.05$ compared to MX solution group.
Abbreviations: BSA, bovine serum albumin; MX, meloxicam; NS, nanosuspension.

To evaluate the effect of the preparation on local inflammatory tissues, an edema assay was conducted. The edema rate was calculated to assess the degree of swelling of rat paw. As the results shown in Figure 10, the edema rates with pretreatment with MX-BSA-NS or MX solution are significantly lower than those of the control groups ($P<0.05$). And the edema rates of the MX-BSA-NS group are higher than those of the MX solution group in the first 2 h, probably due to the immediate release of MX solution. Moreover, the edema rates of MX-BSA-NS group are slightly lower than that of MX solution group after 4 and 6 h, which may be attributed to the targeted delivery and sustained release of MX-BSA-NS. So, it appears that MX-BSA-NS may play an important role in inhibiting paw edema in rats, and its therapeutic effect may be better than MX solution.

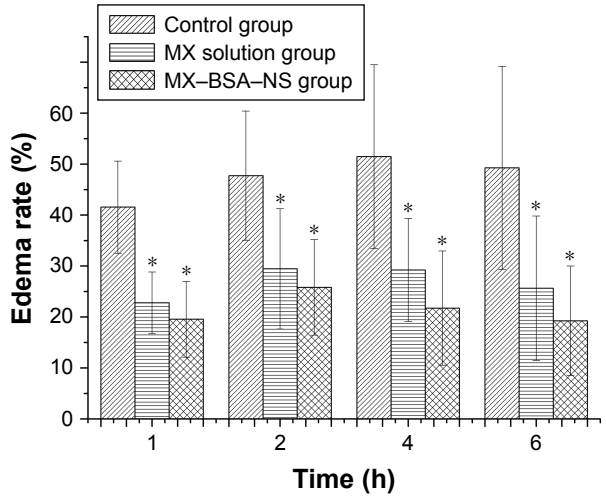

Figure 10 Effects of meloxicam (at an equivalent dose of 25 mg kg^{-1}) on carrageenan-induced paw edema in rats.
Notes: Data are the average values of six experiments (±SD). *$P<0.05$ compared to control group.
Abbreviations: BSA, bovine serum albumin; MX, meloxicam; NS, nanosuspension.

Conclusion

In this study, we demonstrated a simple, feasible preparation technology for preparing a nanosuspension using the method of an acid–base neutralization reaction in aqueous solution. The FTIR spectra showed that BSA was conjugated to the surface of nanoparticles as a stabilizer in the formula. The results of characterization showed that the prepared nanosuspensions had a small size and narrow particle size distribution. In addition, there was no significant change in the appearance, drug content, and particle size of the lyophilized MX-BSA-NS powders during the 6 months of storage period. The physicochemical characteristics of MX-BSA-NS before and after lyophilization were evaluated to confirm the stability of the prepared MX-BSA-NS. In addition, in vitro release experiments revealed that MX-BSA-NS possessed good water solubility and sustained release in comparison with MX solution. A cell viability assay was performed, indicating that the MX nanosuspension and MX solution had similar IC_{50} values. The pharmacokinetic studies showed that there was a long in vivo circulation of prepared nanosuspensions according to the MRT and $t_{1/2}$ results. More importantly, MX-BSA-NS particularly targeted inflammatory sites, producing an improved anti-inflammatory therapeutic effect and increasing the drug bioavailability. Therefore, the acid–base neutralization reaction is a suitable strategy for increasing the solubility of poorly water-soluble drugs with pH-dependent solubility. The MX-BSA-NS delivery system is a promising way for achieving improved therapeutic efficacy and increasing the bioavailability of MX.

Acknowledgments

The authors gratefully acknowledge financial support from the National Natural Science Foundation of People's Republic of China (no 81703709) and the National Natural Science Foundation of People's Republic of China (no 81473163).

Disclosure

The authors report no conflicts of interest in this work.

References

1. Engelhardt G, Homma D, Schlegel K, Utzmann R, Schnitzler C. Anti-inflammatory, analgesic, antipyretic and related properties of meloxicam, a new non-steroidal anti-inflammatory agent with favourable gastrointestinal tolerance. *Inflamm Res*. 1995;44(10):423–433.

2. Elmotasem H. Chitosan–alginate blend films for the transdermal delivery of meloxicam. *Asian J Pharm Sci*. 2008;(1):12–29.
3. Ianiski FR, Alves CB, Ferreira CF, et al. Meloxicam-loaded nanocapsules as an alternative to improve memory decline in an Alzheimer's disease model in mice: involvement of Na(+), K(+)-ATPase. *Metab Brain Dis*. 2016;31(4):793–802.
4. Luger P, Daneck K, Engel W, Trummlitz G, Wagner K. Structure and physicochemical properties of meloxicam, a new NSAID. *Eur J Pharm Sci*. 1996;4(3):175–187.
5. Ah YC, Choi JK, Choi YK, Ki HM, Bae JH. A novel transdermal patch incorporating meloxicam: in vitro and in vivo characterization. *Int J Pharm*. 2010;385(1–2):12–19.
6. Yuan Y, Li SM, Mo FK, Zhong DF. Investigation of microemulsion system for transdermal delivery of meloxicam. *Int J Pharm*. 2006; 321(1–2):117–123.
7. Chen J, Gao Y. Strategies for meloxicam delivery to and across the skin: a review. *Drug Deliv*. 2016;23(8):3146–3156.
8. Farid M, El-Setouhy DA, El-Nabarawi MA, El-Bayomi T. Particle engineering/different film approaches for earlier absorption of meloxicam. *Drug Deliv*. 2016;23(7):2309–2317.
9. Horvath T, Ambrus R, Volgyi G, et al. Effect of solubility enhancement on nasal absorption of meloxicam. *Eur J Pharm Sci*. 2016;95:96–102.
10. Iurian S, Tomuta I, Rus L, Achim M, Leucuta SE. Optimization of the sonication process for meloxicam nanocrystals preparation. *Clujul Med*. 2015;88(3):366–372.
11. Pan S, Takebe G, Suzuki M, et al. Nanonization of poorly water-soluble drug clobetasone butyrate by using femtosecond laser. *Opt Commun*. 2014;313:152–156.
12. Chen H, Khemtong C, Yang X, Chang X, Gao J. Nanonization strategies for poorly water-soluble drugs. *Drug Discov Today*. 2011;16(7–8): 354–360.
13. Li Y, Zhao X, Zu Y, Zhang Y. Preparation and characterization of paclitaxel nanosuspension using novel emulsification method by combining high speed homogenizer and high pressure homogenization. *Int J Pharm*. 2015;490(1–2):324–333.
14. Sattar A, Chen D, Jiang L, et al. Preparation, characterization and pharmacokinetics of cyadox nanosuspension. *Sci Rep*. 2017;7(1):2289.
15. Hu K, Zhou H, Liu Y, et al. Hyaluronic acid functional amphipathic and redox-responsive polymer particles for the co-delivery of doxorubicin and cyclopamine to eradicate breast cancer cells and cancer stem cells. *Nanoscale*. 2015;7(18):8607–8618.
16. Guo M, Law W-C, Ng CH, et al. Preparation of size tunable, glutathione-responsive hyaluronic acid-quantum dot nanohybrids using microemulsion method. *Sci Adv Mater*. 2015;7(2):364–370.
17. Karpel RL, da Silva Liberato M, Campeiro JD, et al. Design and characterization of crotamine-functionalized gold nanoparticles. *Colloids Surf B Biointerfaces*. 2018;163:1–8.
18. Lee SH, Jung HK, Kim TC, et al. Facile method for the synthesis of gold nanoparticles using an ion coater. *Appl Surf Sci*. 2018;434:1001–1006.
19. Chuesiang P, Siripatrawan U, Sanguandeekul R, McLandsborough L, Julian McClements D. Optimization of cinnamon oil nanoemulsions using phase inversion temperature method: impact of oil phase composition and surfactant concentration. *J Colloid Interface Sci*. 2018; 514:208–216.
20. Fang J, Nakamura H, Maeda H. The EPR effect: unique features of tumor blood vessels for drug delivery, factors involved, and limitations and augmentation of the effect. *Adv Drug Deliv Rev*. 2011;63(3):136–151.
21. Guo L, Kang L, Liu X, et al. A novel nanosuspension of andrographolide: preparation, characterization and passive liver target evaluation in rats. *Eur J Pharm Sci*. 2017;104:13–22.
22. Torchilin V. Tumor delivery of macromolecular drugs based on the EPR effect. *Adv Drug Deliv Rev*. 2011;63(3):131–135.
23. Wang L, Du J, Zhou Y, Wang Y. Safety of nanosuspensions in drug delivery. *Nanomedicine*. 2017;13(2):455–469.
24. Yadollahi R, Vasilev K, Simovic S. Nanosuspension technologies for delivery of poorly soluble drugs. *J Nanomater*. 2015;2015:1–13.
25. Maeda H, Matsumura Y. EPR effect based drug design and clinical outlook for enhanced cancer chemotherapy. *Adv Drug Deliv Rev*. 2011; 63(3):129–130.
26. Chen C, Hu H, Qiao M, et al. Tumor-targeting and pH-sensitive lipoprotein-mimic nanocarrier for targeted intracellular delivery of paclitaxel. *Int J Pharm*. 2015;480(1–2):116–127.
27. Wang Z, Li Z, Zhang D, Miao L, Huang G. Development of etoposide-loaded bovine serum albumin nanosuspensions for parenteral delivery. *Drug Deliv*. 2015;22(1):79–85.
28. Kaya M, Mulercikas P, Sargin I, et al. Three-dimensional chitin rings from body segments of a pet diplopod species: characterization and protein interaction studies. *Mater Sci Eng C Mater Biol Appl*. 2016; 68:716–722.
29. Kratz F. Albumin as a drug carrier: design of prodrugs, drug conjugates and nanoparticles. *J Control Release*. 2008;132(3):171–183.
30. Rahimnejad MM, Jahanshahi M, Najafpour GD. Production of biological nanoparticles from bovine serum albumin for drug delivery. *Afr J Biotechnol*. 2010;5(20):1918–1923.
31. Ledesma AE, Chemes DM, Frías MdlA, Guauque Torres MdP. Spectroscopic characterization and docking studies of ZnO nanoparticle modified with BSA. *Appl Surf Sci*. 2017;412:177–188.
32. Rubino OP, Kowalsky R, Swarbrick J. Albumin microspheres as a drug delivery system: relation among turbidity ratio, degree of cross-linking, and drug release. *Pharm Res*. 1993;10(7):1059–1065.
33. Du T, Liu B, Hou X, Zhang B, Du C. Covalent immobilization of glucose oxidase onto Poly(St-GMA-NaSS) monodisperse microspheres via BSA as spacer arm. *Appl Surf Sci*. 2009;255(18):7937–7941.
34. Jadhav PD, Shim YY, Reaney MJ. Synthesis and characterization of site-selective orbitide-BSA conjugate to produce antibodies. *Bioconjug Chem*. 2016;27(10):2346–2358.
35. Garcia DR, Lavignac N. Poly(amidoamine)–BSA conjugates synthesised by Michael addition reaction retained enzymatic activity. *Polym Chem*. 2016;7(47):7223–7229.
36. Han M, Liu X, Guo Y, Wang Y, Wang X. Preparation, characterization, biodistribution and antitumor efficacy of hydroxycamptothecin nanosuspensions. *Int J Pharm*. 2013;455(1–2):85–92.
37. Kim TH, Jiang HH, Youn YS, et al. Preparation and characterization of water-soluble albumin-bound curcumin nanoparticles with improved antitumor activity. *Int J Pharm*. 2011;403(1–2):285–291.
38. Gawde KA, Kesharwani P, Sau S, et al. Synthesis and characterization of folate decorated albumin bio-conjugate nanoparticles loaded with a synthetic curcumin difluorinated analogue. *J Colloid Interface Sci*. 2017;496:290–299.
39. Ahuja BK, Jena SK, Paidi SK, Bagri S, Suresh S. Formulation, optimization and in vitro-in vivo evaluation of febuxostat nanosuspension. *Int J Pharm*. 2015;478(2):540–552.
40. Mou D, Chen H, Wan J, Xu H, Yang X. Potent dried drug nanosuspensions for oral bioavailability enhancement of poorly soluble drugs with pH-dependent solubility. *Int J Pharm*. 2011;413(1–2):237–244.
41. Zhao X, Wang W, Zu Y, et al. Preparation and characterization of betulin nanoparticles for oral hypoglycemic drug by antisolvent precipitation. *Drug Deliv*. 2014;21(6):467–479.
42. Xu Y, Liu X, Lian R, et al. Enhanced dissolution and oral bioavailability of aripiprazole nanosuspensions prepared by nanoprecipitation/homogenization based on acid-base neutralization. *Int J Pharm*. 2012; 438(1–2):287–295.
43. Sadeghi H, Hajhashemi V, Minaiyan M, Movahedian A, Talebi A. Further studies on anti-inflammatory activity of maprotiline in carrageenan-induced paw edema in rat. *Int Immunopharmacol*. 2013; 15(3):505–510.
44. Elzoghby AO, Samy WM, Elgindy NA. Albumin-based nanoparticles as potential controlled release drug delivery systems. *J Control Release*. 2012;157(2):168–182.
45. Chen H, Wan J, Wang Y, et al. A facile nanoaggregation strategy for oral delivery of hydrophobic drugs by utilizing acid-base neutralization reactions. *Nanotechnology*. 2008;19(37):375104.

46. Ali HS, York P, Blagden N. Preparation of hydrocortisone nanosuspension through a bottom-up nanoprecipitation technique using microfluidic reactors. *Int J Pharm*. 2009;375(1–2):107–113.
47. Patravale VB, Date AA, Kulkarni RM. Nanosuspensions: a promising drug delivery strategy. *J Pharm Pharmacol*. 2004;56(7):827–840.
48. Jensen LG, Skautrup FB, Mullertz A, Abrahamsson B, Rades T, Priemel PA. Amorphous is not always better: a dissolution study on solid state forms of carbamazepine. *Int J Pharm*. 2017;522(1–2):74–79.
49. Singh S, Vaidya Y, Gulati M, Bhattacharya S, Garg V, Pandey N. Nanosuspension: principles, perspectives and practices. *Curr Drug Deliv*. 2016;13(8):1222–1246.
50. Gao L, Zhang D, Chen M. Drug nanocrystals for the formulation of poorly soluble drugs and its application as a potential drug delivery system. *J Nanopart Res*. 2008;10(5):845–862.
51. Maeda H, Nakamura H, Fang J. The EPR effect for macromolecular drug delivery to solid tumors: improvement of tumor uptake, lowering of systemic toxicity, and distinct tumor imaging in vivo. *Adv Drug Deliv Rev*. 2013;65(1):71–79.

Supplementary materials

Table S1 Summary of the experiments performed

Experiment	Content of Tween-80 (w/v) (%)	MX:BSA	Content of MX (mg mL^{-1})	Particle size (nm)	Particle size after 24 h (nm)	Stability time (at 4°C)
1	0.1	1:5	5	255.5	592.3	ND
2	0.2	1:5	5	179.4	445.6	ND
3	0.3	1:5	5	78.42	78.61	>15 days
4	0.4	1:5	5	71.5	187.9	ND
5	0.3	1:1	5	90.12	Precipitation appeared	<1 day
6	0.3	1:3	5	87.82	114.37	3 days
7	0.3	1:10	5	108.17	139.25	3 days
8	0.3	1:7	5	85.81	90.49	7 days
9	0.3	1:5	2.5	92.35	ND	>15 days
10	0.3	1:5	7.5	59.21	ND	<3 days

Note: Stability time: the time that precipitation did not appear.
Abbreviations: BSA, bovine serum albumin; MX, meloxicam; ND, not determined.

Table S2 Solubility of MX in different media (37°C±0.5°C)

Medium	Solubility (mg mL^{-1})
Distilled water	0.0079
0.1 mol L^{-1} HCl	0.0013
0.01 mol L^{-1} HCl	0.0019
pH 4.0 PBS	0.0034
pH 5.0 PBS	0.0055
pH 5.8 PBS	0.0183
pH 6.5 PBS	0.1630
pH 7.4 PBS	0.6403
pH 8.5 PBS	1.5502
10^{-4} mol L^{-1} NaOH	2.0568
10^{-3} mol L^{-1} NaOH	3.1594
0.01 mol L^{-1} NaOH	3.6188
0.1 mol L^{-1} NaOH	32.4790
0.4 mol L^{-1} NaOH	5.4864

Abbreviation: MX, meloxicam.

Table S3 The appearance of formulations containing different cryoprotectants

Cryoprotectants	3% (w/v)	5% (w/v)	7% (w/v)	10% (w/v)
None	+	+	+	+
Glucose	–	–	–	–
Sucrose	–	–	–	–
Lactose	–	–	–	+
Trehalose	–	–	–	–
Mannitol	+	+	+	+
Maltose	–	–	–	–

Notes: +, smooth and compact; –, collapse.

Table S4 Reconstitution of various cryoprotectants on the character of the freeze-dried product

Cryoprotectants	3% (w/v)	5% (w/v)	7% (w/v)	10% (w/v)
None	+	+	+	+
Glucose	–	–	–	–
Sucrose	–	–	–	–
Lactose	–	–	–	–
Trehalose	+	–	–	–
Mannitol	+	++	++	+
Maltose	–	–	–	–

Notes: ++, translucent; +, opalescent; –, milky or sedimentary.

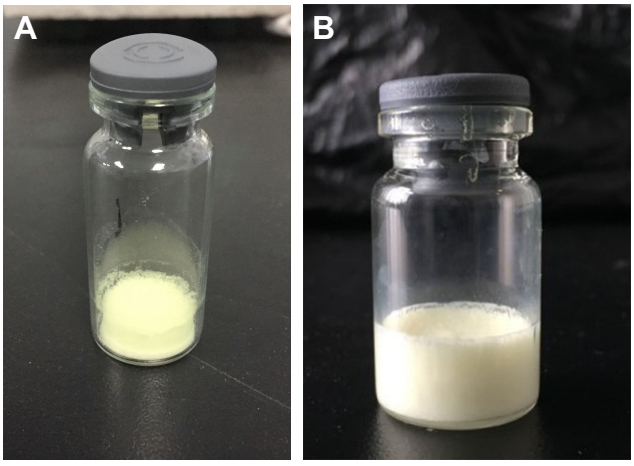

Figure S1 The collapsed (**A**) and smooth and compact (**B**) appearances of freeze-dried products containing different cryoprotectants.

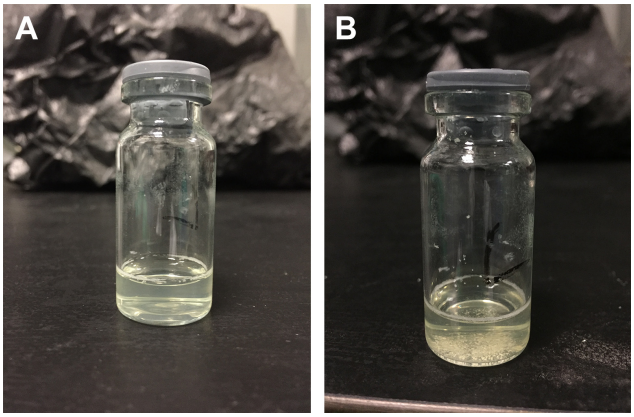

Figure S2 Appearance of MX nanosuspension without BSA coating before (**A**) and after (**B**) 24 h of placement.
Abbreviations: BSA, bovine serum albumin; MX, meloxicam.